

Influence of fault zone maturity on fully dynamic earthquake cycles

Prithvi Thakur¹ and Yihe Huang¹

¹University of Michigan, Department of Earth and Environmental Sciences

Key Points:

- We simulate earthquake cycles in fault zones with coseismic damage and interseismic healing.
- There are more surface-rupturing events with regular recurrence intervals as the modeled fault zones become more mature.
- Healing in immature fault zone models promotes slow-slip events within the seismogenic zone causing partial ruptures.

Corresponding author: Prithvi Thakur, prith@umich.edu

This is the author manuscript accepted for publication and has undergone full peer review but has not been through the copyediting, typesetting, pagination and proofreading process, which may lead to differences between this version and the [Version of Record](#). Please cite this article as doi: [10.1029/2021GL094679](https://doi.org/10.1029/2021GL094679).

This article is protected by copyright. All rights reserved.

Abstract

We study the mechanical response of two-dimensional vertical strike-slip fault to coseismic damage evolution and interseismic healing of fault damage zones by simulating fully dynamic earthquake cycles. Our models show that fault zone structure evolution during the seismic cycle can have pronounced effects on mechanical behavior of locked and creeping fault segments. Immature fault damage zone models exhibit small and moderate subsurface earthquakes with irregular recurrence intervals and abundance of slow-slip events during the interseismic period. In contrast, mature fault damage zone models host pulse-like earthquake ruptures that can propagate to the surface and extend throughout the seismogenic zone, resulting in large stress drop, characteristic rupture extents, and regular recurrence intervals. Our results suggest that interseismic healing and coseismic damage accumulation in fault zones can explain the observed differences of earthquake behaviors between mature and immature fault zones and indicate a link between regional seismic hazard and fault structural maturity.

Plain Language Summary

Fault zones are geometrically complex network of fractures with slip surfaces that are capable of hosting earthquakes. This network evolves through time as more and more earthquakes generate damage in the vicinity of the slip surfaces. We use numerical models to simulate different stages of fault-slip behavior including earthquakes, slow-slip events, and aseismic creep on a planar fault surrounded by a damage zone. This damage zone is prescribed to accumulate damage after an earthquake and heal during the quiet periods between earthquakes. Depending on the compliance (i.e., the ability to accommodate deformation) of the damage zone with respect to the surrounding host rock, a fault zone can be at different stages of its maturity, with higher compliance corresponding to a more mature fault zone. We find that our models with immature fault zone tends to produce smaller earthquakes whose slip does not reach the surface of the earth, and the duration between earthquakes is irregular. As fault zones become more mature in the models, earthquakes can rupture to the surface and occur more regularly. Our results highlight a link between regional seismic hazard and fault structural maturity.

1 Introduction

Active faults are usually surrounded by narrow regions of localized deformation extending several hundred meters to a few kilometers in width across the fault. This deformation zone consisting of a dense fracture network is macroscopically viewed as an elastic layer with low seismic wave velocities and referred to as a fault damage zone (Ben-Zion & Sammis, 2003). The strength of the fault damage zone evolves throughout the seismic cycle, but the details of the evolution mechanism and the nature of this evolution remain elusive.

Fault zone maturity can be defined and quantified by the total slip accumulated over time in field geologic and geodetic studies (Dolan & Haravitch, 2014), with larger slip corresponding to higher maturity. Figure 1 shows a conceptual model of how a strike-slip fault system may evolve through multiple earthquake cycles. Immature fault zones (Figure 1a) are characterized by a distributed network of damage, and as the fault zone matures (Figure 1c), the damage becomes localized. The faulting itself becomes more localized, transitioning from multiple and discontinuous slip surfaces to a more throughgoing fault. Other parameters such as the total fault length, the slip rate, and the initiation age have also been used to determine fault zone maturity (Perrin et al., 2016). However, the surface slip expression for immature faults usually underestimate slip at depth by about 10% to 60% (Dolan & Haravitch, 2014). Perrin et al. (2016) have shown that structural maturity of a strike-slip fault zone is well correlated with the seismic wave velocity of near-fault materials, which decreases as the fault zone becomes progressively more mature. Such

61 velocity reductions are well documented along mature fault zones such as the San Andreas
62 fault zone (Y.-G. Li et al., 2006a; M. A. Lewis & Ben-Zion, 2010), San Jacinto fault zone
63 (M. Lewis et al., 2005), Nojima fault zone (Mizuno et al., 2008), and Wenchuan fault zone
64 (Pei et al., 2019). Examples of immature fault zones that exhibit less evidence of localized
65 damage include the northern part of the San Andreas fault zone (Waldhauser & Ellsworth,
66 2002), the Bam fault in Iran (Fielding et al., 2009), the Jiuzhaigou earthquake near Kunlun
67 fault zone in China (Y. Li et al., 2020), and Peloponnese fault zone in Greece (Feng et al.,
68 2010). Previous studies have shown that a more compliant or mature fault damage zone
69 enables ruptures to propagate as slip pulses (Harris & Day, 1997; Huang & Ampuero, 2011a;
70 Huang et al., 2014a; Thakur et al., 2020; Idini & Ampuero, 2020b). Geodetic observations
71 (e.g., Goldberg et al. (2020); Feng et al. (2010)) have shown earthquake slip distributions
72 are complex in an immature fault zone, and they become more uniform as the fault zone
73 matures. Understanding the long-term earthquake behavior during the structural evolution
74 of the fault damage zone is key to unraveling the locations, recurrence intervals, stressing
75 history, and the probability of subsequent earthquakes in an active fault zone.

76 Observations of seismic wave velocity changes within the fault damage zone (< 1 km
77 from the fault; e.g., Vidale and Li (2003); Y.-G. Li et al. (2003, 2006a); Wu et al. (2009);
78 Peng and Ben-Zion (2006); Zhao and Peng (2009); Roux and Ben-Zion (2014)) documented
79 a sharp decrease in pressure- and shear-wave velocities following earthquakes as well as a
80 subsequent logarithmic increase in wave velocity with time. Other observations further away
81 from the fault zone (e.g., Taira et al. (2009); Chen et al. (2015); Pei et al. (2019)) revealed
82 coseismic reduction and interseismic increase of seismic wave velocities in the surround-
83 ing region. Laboratory experiments have shown similar change in seismic wave velocities
84 (P. A. Johnson & Jia, 2005; Kaproth & Marone, 2014; Snieder et al., 2016) wherein they
85 observe compaction during holds (i.e., interseismic period) and dilation during fault slip
86 (i.e., seismic events). Mechanisms for damage accumulation in active fault zones are likely
87 a combination of processes including dilation, compaction, cracking, shear driven pulveriza-
88 tion, and fabric generation (Gratier et al., 2003). The observed coseismic seismic velocity
89 drop is potentially related to brecciation, cataclasis, and damage accumulation, implying a
90 magnitude dependence of this velocity drop (Y.-G. Li et al., 2003; Rubinstein & Beroza,
91 2005; Brenguier et al., 2008).

92 During the interseismic period, time-dependent fault zone healing may occur due to a
93 combination of rheological restrengthening, inelastic strain, mineral precipitation, and fluid
94 pressure recovery (Vidale & Li, 2003). There is some debate on whether this healing time is
95 significant in contributing to fault zone stress redistribution and therefore influencing long-
96 term seismicity (Vidale & Li, 2003; Mizuno et al., 2008). It is hard to accurately quantify
97 fault zone healing time because it requires long-term continuous monitoring of seismic wave
98 velocities. Active seismic studies along the Landers fault zone (Vidale & Li, 2003) and
99 Longmenshan fault zone (Pei et al., 2019) suggest that it may take years or decades to
100 heal completely, whereas other studies (Peng & Ben-Zion, 2006; Mizuno et al., 2008; Wu
101 et al., 2009) suggest that the healing time may not be longer than the typical timescales of
102 postseismic afterslip, i.e., a couple of months. Another study by Roux and Ben-Zion (2014)
103 along the North Anatolian Fault suggests a recovery rate over a timescale of few days. It
104 is worthwhile noting that some of these studies may have a lower spatial resolution than
105 others which might affect the inference of fault zone recovery rate.

106 We use numerical simulations to understand the effects of fault zone damage accumu-
107 lation after multiple cycles of earthquakes and healing during the interseismic period on a
108 two-dimensional vertical strike-slip fault. We model the fault zone structure evolution as
109 changes in the shear wave velocity of an elastic layer surrounding a strike-slip fault. This
110 elastic fault damage zone has a lower shear wave velocity, and therefore, a lower rigidity
111 compared to the surrounding host rock. We assume a constant density in our numerical sim-
112 ulations as the changes in shear-wave velocity has a more significant effect on the rigidity of
113 the material. Throughout the remainder of this article, we will use the term "rigidity ratio",

114 which is the percentage ratio of the fault zone shear modulus to the host rock shear modulus,
 115 to parameterize the fault zone evolution through time. Figure 1b shows a representative
 116 rigidity ratio evolution through time. We constrain the coseismic damage accumulation and
 117 the rate of interseismic healing using shear-wave velocity observations from Wenchuan (Pei et
 118 al., 2019), Landers (Vidale & Li, 2003), Nojima (Mizuno et al., 2008), and North Anatolian
 119 Fault zones (Peng & Ben-Zion, 2006). We describe the numerical procedure and the fault
 120 zone healing mechanism in section 2 and Supporting Information. The results of our models
 121 are described in section 3. We show that an immature fault zone tends to produce more
 122 slow-slip events and irregular earthquake sequences with predominantly subsurface events.
 123 In contrast, a more mature fault damage zone tends to produce a more regular sequence
 124 of earthquakes with a combination of surface-reaching and subsurface events. In section 4,
 125 we discuss the implications of our results for earthquake cycle behaviors of strike-slip fault
 126 zones.

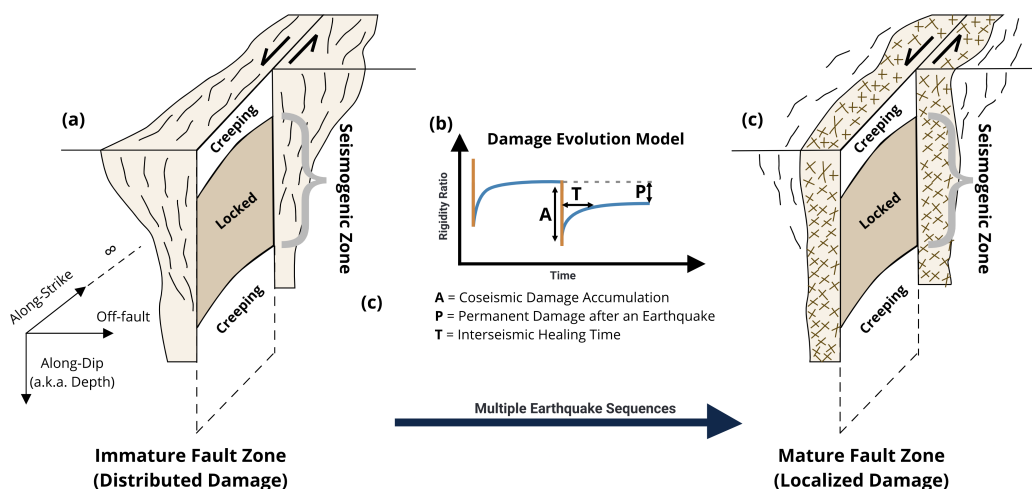


Figure 1. A conceptualized evolution of a fault damage zone through multiple earthquake sequences for strike-slip fault systems. (a) Schematic of an immature fault zone with distributed damage increases towards the surface. (b) Parameters considered for an elastic damage evolution model, showing the prescribed change in the rigidity ratio (ratio of shear modulus in damage zone to that in the host rock) through time. (c) Schematic of a mature fault zone with localized damage and a dense fracture network.

127 2 Model Description

128 We use two-dimensional earthquake cycle models of strike-slip faults with mode III rupture
 129 where the displacement is out of the plane of interest and stresses and friction vary with
 130 depth. For simplicity, we use a narrow fault-parallel layer as a proxy for the damage zone
 131 and its geometry remains constant throughout the simulated sequence. This is equivalent
 132 taking a vertical cross-section across Figure 1c, and the fault zone maturity in the damage
 133 evolution model corresponds to the change in rigidity ratio without changing the geometry
 134 of the fault zone (Figure 1b). The frictional properties and initial conditions are chosen to
 135 keep the frictional complexities at a minimum (See Supporting Information). Here we focus
 136 the discussion on fault zone properties.

137 Since there are very few long-term observations (10,000-100,000 years) documenting
138 the changes in permanent damage through multiple earthquake cycles, we limit ourselves
139 to modeling short earthquake sequences for several hundred years each, with each sequence
140 intended to represent different stages of fault zone maturity, including an immature stage
141 and a mature stage, both of which accumulate no permanent damage. We also consider
142 a transition stage which incorporates permanent damage, i.e., a reduction in rigidity after
143 each earthquake. The distinction between immature and mature fault zones in our models
144 depends on the rigidity ratio of the damage zone to the host rock. Typically, larger velocity
145 reductions (35 % to 50 %) and lower rigidities (25 % to 45 % of host rock) are measured
146 around mature fault zones, whereas smaller velocity reductions (8 % to 10 %) and higher
147 rigidities (80 % to 90 % of host rock) are measured around immature fault zones (Perrin et
148 al., 2016). Based on these seismic wave velocity measurements, we choose a rigidity ratio
149 changing between 80 % and 85 % of host rock for the immature fault zone and a rigidity
150 ratio changing between 40 % and 45 % of the host rock for the mature fault zone. While
151 mature fault zones can have lower rigidities as well, the chosen values lie well within what
152 is observed for mature and immature fault zones.

153 Another important parameter is the coseismic velocity drop. While its value is not
154 well constrained by observations and can vary significantly (0.1 % to 5 %) between different
155 fault zones such as Parkfield (Y.-G. Li et al., 2006a), Wenchuan (Pei et al., 2019), and
156 Landers (Y.-G. Li et al., 2003), it is dependent on the size of the earthquake with smaller
157 earthquakes showing smaller coseismic drop. Since our simulations are two-dimensional
158 and do not have any along-strike constraints on the earthquake size, we use a magnitude-
159 independent coseismic damage accumulation of 5 % rigidity change in order to facilitate a
160 better comparison between different simulation cycles.

161 Our current models are a purely elastic approximation of how a fault damage zone
162 may evolve over time through multiple earthquake sequences. This ignores the energy dis-
163 sipated through the damage process (e.g., (Okubo et al., 2019)), including that required for
164 secondary crack formation (Lyakhovsky et al., 2005). Additionally, the coseismic velocity
165 drop in our models approximates the damage evolution and crack propagation over smaller
166 timescales during each event to a step change that occurs after the event is over. Other
167 plausible mechanisms such fault roughness evolution (Heimisson, 2020), or alternate model-
168 ing approaches such as elastic impact (Tsai & Hirth, 2020) might influence the dynamics of
169 earthquake sequences. While incorporating these complexities may affect the overall fault
170 slip behavior, they are computationally very expensive to implement and beyond the scope
171 of the current study.

172 **3 Results**

173 We have tested a range of parameters in our simulations that account for fault zone maturity,
174 coseismic damage accumulation, and healing time. Here the fault zone maturity can be
175 described by the initial rigidity ratio (Figure 1b). These parameters are discussed in the
176 Supporting Information. For brevity, we choose to show representative cases for a healing
177 time of 8 years and a coseismic velocity drop of 5 % in the following subsections. Changing
178 these parameters (e.g., healing time between 1 and 20 years) have some effects on the
179 location and timing of individual earthquakes but does not affect the overall interpretation
180 of our results.

181 **3.1 Effects of fault damage zone maturity**

182 The initial rigidity ratio of fault damage zones with respect to the surrounding host rock
183 can have significant effects on seismicity evolution. A higher initial rigidity ratio implies a
184 less mature fault zone and vice versa. While keeping the permanent damage at zero, we
185 compare an immature fault zone evolution characterized by rigidity ratio changing between
186 80 % and 85 %, against a mature fault zone evolution characterized by rigidity ratio changing

187 between 40% and 45% (Figures 2a and b). For the sake of simplicity, the fault zone
188 accumulates damage by the same amount irrespective of the earthquake size.

189 For the models with a constant healing time, a mature fault zone tends to show more
190 regular earthquake sequences with full (surface-reaching) ruptures, whereas a less mature
191 fault zone shows irregular earthquake sequences with partial (subsurface) ruptures and more
192 slow-slip events (Figures 2c and d). The cumulative slip demonstrates events with variable
193 sizes and depths throughout the seismogenic zone, but we do not see ruptures spanning the
194 entire seismogenic region in the immature fault zone. Instead, we only see ruptures extending
195 across a fraction of the seismogenic zone, and these partial ruptures persist throughout
196 multiple seismic cycles. This phenomenon of partial ruptures occurs only in immature
197 fault zone model with healing, which tend to have crack-like ruptures and overall lower slip
198 velocities. In contrast, mature fault zone model exhibit higher slip-velocities and pulse-like
199 ruptures, which tend to produce surface-reaching ruptures. Such pulse-like ruptures can
200 be identified by looking at the cumulative slip of earthquake cycles in mature fault zones
201 (Figure 2d), where the final slip distribution is nearly flat, a characteristic of pulse-like
202 ruptures (Heaton, 1990).

203 We measure shear stress before and after a representative earthquake from each of
204 these simulations to understand the depth distribution of stress drop and the mechanisms
205 accounting for different earthquake behaviors in mature and immature fault zones. Figures
206 2e and f show the depth distribution of shear stress for an earthquake in the immature and
207 mature fault zone models, respectively. We see that the mature fault zone model exhibits
208 a large, uniform stress drop along the fault dip (Figure 2f) such that stress peaks after the
209 earthquake are concentrated only towards the edges of the velocity-weakening segment due
210 to ruptures propagating throughout the seismogenic zone. On the other hand, the immature
211 fault zone model (Figure 2e) results in a partial stress drop as the rupture is arrested before
212 reaching the edges of the asperity. In this context, a partial stress drop refers to the stresses
213 being released only in a small portion of the velocity-weakening segment along the fault.
214 The partial stress drop in immature fault zones leads to residual stress peaks concentrated
215 within the velocity-weakening region, which may cause subsequent ruptures or slow-slip
216 events near those stress peaks. As discussed in more detail in section 3.2, the slow-slip
217 events can delay the next earthquake rupture and result in irregular recurrence intervals
218 between earthquakes.

219 We also include permanent damage after each earthquake in our model to demonstrate
220 the transition from an immature fault zone to a mature fault zone (i.e., P is nonzero in
221 Figure 1b). While faults in nature need several tens of thousands of years to transition from
222 immature to mature stages, it is not computationally feasible to perform such simulations
223 with full inertial effects. The choice of the amount of coseismic velocity reduction and inter-
224 seismic healing in our simulations allows the transition from immature to mature fault zones
225 within 300-400 years. Figure S1 shows the accumulated slip contours for the earthquake
226 cycle in this scenario. We begin with an initial rigidity ratio of 90% and drop it down by 5%
227 after each earthquake (Figure S1). We allow the fault to recover 80% of the coseismic drop
228 in rigidity during the interseismic period therefore accommodating a permanent damage
229 of 1% rigidity reduction after each earthquake, though smaller recovery percentages may
230 be achieved if the next earthquake occurs before the fault has healed completely (Figure
231 S1b). We see a progressive increase in the rupture length from partial to full ruptures as the
232 fault zone becomes more mature (Figure S1a). We distinguish between an immature and a
233 mature fault damage zone based on when we start observing surface-reaching events that
234 rupture the entire seismogenic zone. Surface-reaching ruptures become prevalent when the
235 rigidity ratio falls below 60% of the host rock. Furthermore, earthquakes become more reg-
236 ular and frequent as the fault zone matures. This simulation informs us that the transition
237 from immature to mature fault zone is gradual, and we can see a mixture of surface-reaching
238 and subsurface events during this transition stage.

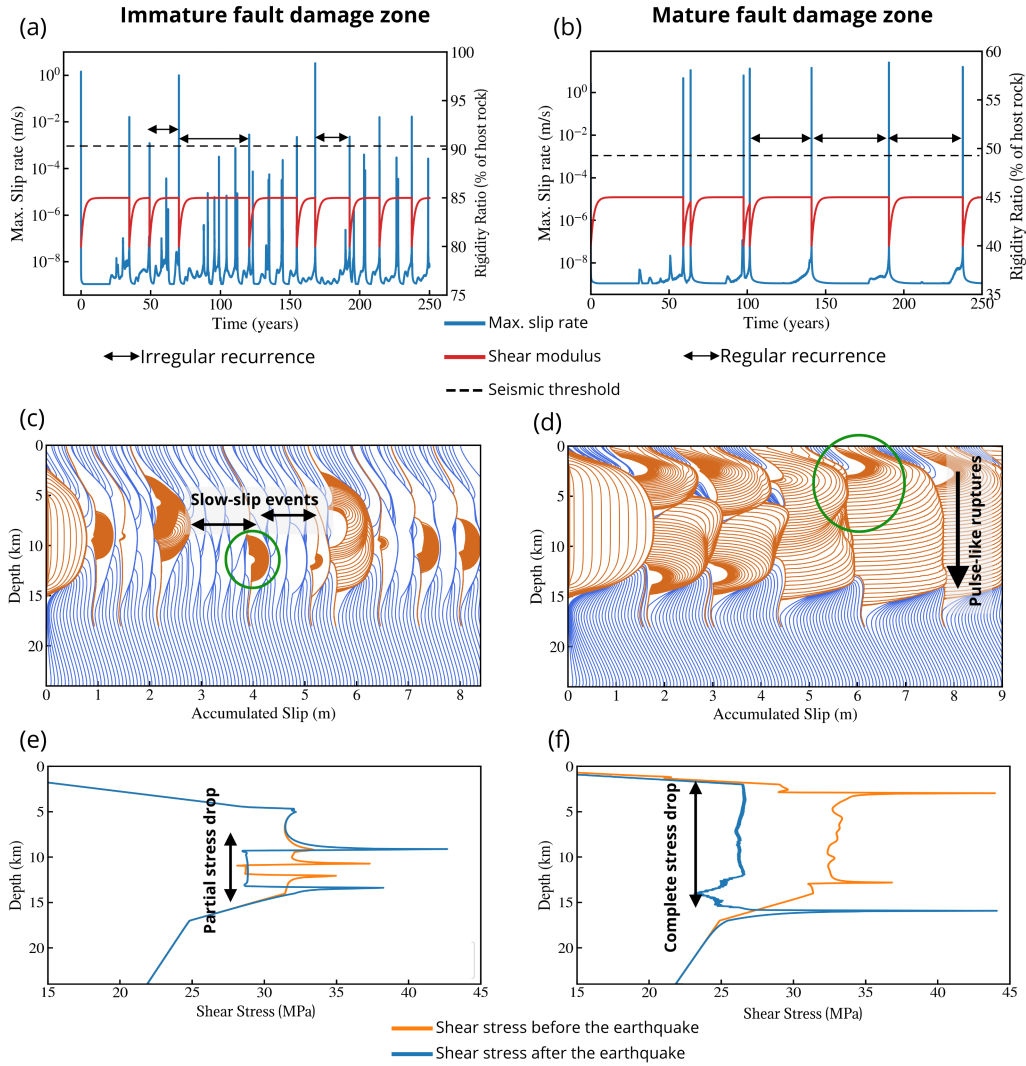


Figure 2. Immature vs mature fault damage zone. (a-b) The evolution of slip-rate function (blue) and the rigidity ratio (red) through time. (c-d) Cumulative slip through earthquake sequences shown along depth in mature and immature fault zones. The orange lines are plotted every 0.1 seconds during earthquakes, and the blue lines are plotted every year during interseismic periods. (e-f) The on-fault shear stress before and after a representative earthquake for each case (circled in green in (c) and (d)) demonstrates a partial stress-drop for immature fault zones and a complete stress drop for mature fault zones.

3.2 Effects of healing: slow-slip events and irregularity in recurrence intervals

Interseismic healing has significant effects on the dynamics of earthquakes and aseismic fault-slip, including creep accumulation within the nominally velocity-weakening region, inhibition of surface-reaching events, restriction of earthquake sizes, and generation of slow-slip events also within the velocity-weakening region. Here we discuss the effects of healing

245 in an immature fault zone in more detail and demonstrate how slow-slip events affect seis-
246 micity by comparing a simulation with fault zone rigidity ratio ranging between 60 % and
247 65 % against a fault zone with the same initial rigidity ratio but without healing (i.e., a
248 constant rigidity ratio of 60 %). This range of rigidity ratio still lies in the immature fault
249 zone parameter space discussed in the previous section but leads to fewer slow-slip events
250 compared to the 80 % to 85 % range. It allows us to analyze the healing effect and slow-slip
251 events more clearly.

252 In our numerical simulations, slow-slip events are manifested as accelerated slip that
253 fail to reach the seismic threshold velocity but release finite stress on the slip patch along
254 a portion of the fault. The slip rate of slow slip events in our simulations can vary from
255 $1 \times 10^{-8} \text{ m s}^{-1}$ to $1 \times 10^{-4} \text{ m s}^{-1}$ (Figure 3). Besides slow-slip events, the events below the
256 seismic threshold in our simulations also encompass aseismic creep and afterslip (Figure
257 3b). Aseismic creep is characterized by slip rate that is close to the tectonic plate rate (\leq
258 $1 \times 10^{-9} \text{ m s}^{-1}$). Afterslip is another category of transient slow-slip that releases stresses
259 from recent earthquakes during the postseismic stage (Avouac, 2015; Bürgmann, 2018). The
260 slip rate of afterslip is typically below the seismic slip rate of 1 mm s^{-1} and can go down to
261 $1 \times 10^{-5} \text{ m s}^{-1}$. Afterslip can be distinguished from the slow-slip events by when and where
262 they occur, i.e., away from peak-slip regions of earthquakes.

263 Figures 3a and b show the slip-rate evolution for a fault zone without and with healing
264 during the seismic cycle. The simulation without healing (Figure 3a) shows large surface-
265 reaching ruptures that are periodic in time. This sequence of earthquakes encompasses
266 dynamic events and aseismic creep but does not exhibit any slow-slip events between them.
267 Figure 3b shows a wider range of events including multiple slow-slip events in addition
268 to earthquakes and creep. Such slow-slip events can be identified from the peak slip-rate
269 function in these simulations (Figures 2a and b, and Figure 3d) and generally occur during
270 the interseismic stage within the seismogenic zone in our simulations (Figures 3b and d).
271 These slow-slip events are distributed throughout the interseismic period, with no temporal
272 preference before or after an earthquake, though they have a spatial preference in relation to
273 the residual stresses from previous events. Earthquake ruptures and slow-slip events in our
274 simulations with fault zone healing occur at the edges of previous ruptured region within
275 the velocity-weakening zone (Figure 3b), due to residual stress peaks from those events. The
276 slow-slip events also contribute to the release of stresses during the interseismic period, and
277 in addition, generate stress-peaks within the seismogenic zone, away from its base. This
278 is in contrast to the simulation without healing (Figure 3a), where the stress peaks are
279 predominantly near the base of the seismogenic zone. Other numerical studies (Barbot,
280 2019c; Idini & Ampuero, 2020b) also showed that slow-slip events can be generated in the
281 velocity-weakening part of the fault using quasi-dynamic continuum models. However, the
282 relative size of seismogenic asperity to nucleation, R_u (Barbot, 2019b), for such simulations
283 is much lower than what we use here. Such numerical simulations can exhibit periodic slow-
284 slip events at lower R_u values (< 1) and chaotic slow-slip events at higher R_u values (> 13).
285 Our simulations use an $R_u \sim 5$, which should result in periodic bilateral ruptures, as seen in
286 Figure 3a. Note that the incorporation of healing does not change the R_u values significantly
287 as they lie in the same parameter regime through time. However, interseismic healing helps
288 release the stresses inelastically through time during the quasi-static deformation, which
289 rearranges the stress-peaks and stress shadows along the fault dip, resulting in restriction
290 of earthquake sizes and generation of slow-slip events.

291 Since the interseismic healing promotes slow-slip events, stresses are released nonuni-
292 formly along the fault during this period. This causes partial ruptures to terminate without
293 reaching the free surface. Moreover, these slow-slip events delay the onset of subsequent
294 earthquakes. We see in Figures 3d and f that earthquakes become farther apart in time when
295 there are slow-slip events between them, as compared to consecutive earthquakes occurring
296 without such slow-slip events. This delay, combined with the occurrence of slow-slip events
297 within the velocity-weakening region, gives rise to the irregular recurrence of earthquakes

298 in immature fault zones with healing. We can also infer that the slow-slip events with
 299 higher amount of slip release more stresses during the interseismic period, which delays the
 300 subsequent earthquake by a larger amount (Figure 3f).

301 Another notable feature of the simulation with healing is the penetration of aseismic
 302 creep into the velocity-weakening part of the fault (Figure 3b). The simulation without
 303 healing (Figures 3a and c) shows complete ruptures with regular recurrence intervals, and
 304 aseismic creep is constrained to the velocity-strengthening parts of the fault. However, the
 305 incorporation of healing during the interseismic period allows the creep to accumulate and
 306 build up progressively within the velocity-weakening region (Figures 3b and d). We demon-
 307 strate the cumulative rupture and creep extent from all the events in our simulation with
 308 healing in relation to the velocity weakening and velocity strengthening regions along the
 309 fault on the right side of Figure 3b. We see that the cumulative creep extends through
 310 almost the entire fault, whereas the earthquake rupture extent is predominantly confined
 311 to the velocity weakening region. Creeping within the seismogenic zone also causes nonuni-
 312 form stress release during the interseismic period, similar to the effects of slow-slip events
 313 discussed above, albeit to a lesser extent.

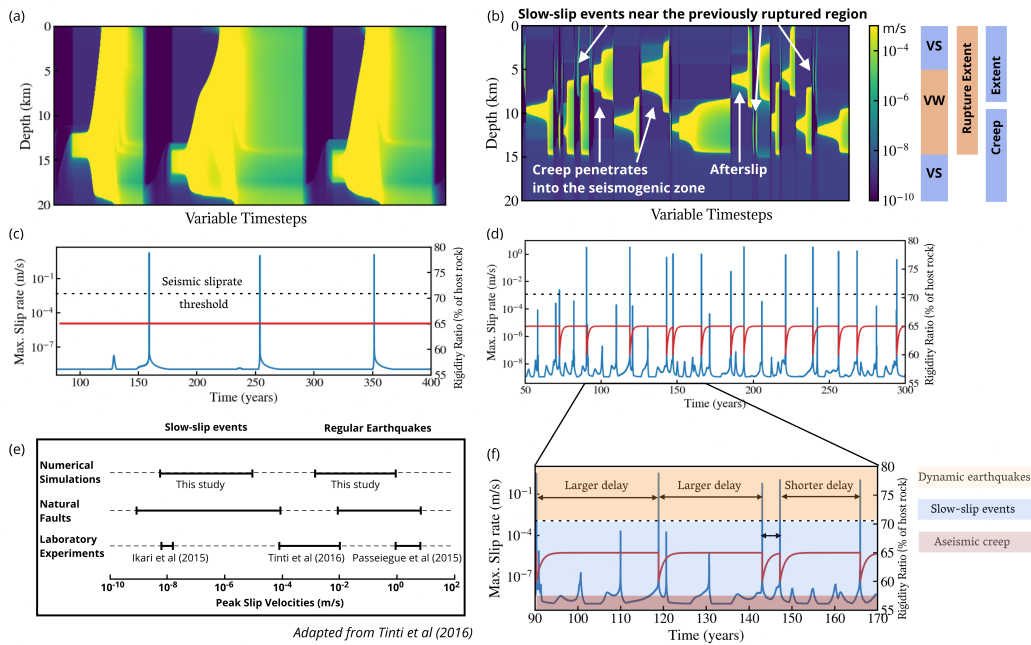


Figure 3. (a) The spatiotemporal slip-rate evolution in immature fault zone without healing (see color scale in (b)). (b) The spatiotemporal slip-rate evolution in immature fault zone with healing. The right side shows the depth extent of the frictional parameters delineating the velocity-weakening and the velocity-strengthening region. (c-d) The rigidity ratio and the peak slip-rate function for a segment of the simulation. (e) A compilation of the peak slip-velocity range for slow-slip events from laboratory experiments, natural faults, and our numerical simulations. (f) Zoom in of part (d), showing larger delay in earthquake onset for higher slow slip-rates.

314 This effect of creep buildup within the velocity-weakening region and the abundance
 315 of slow-slip events is also observed in our simulation with permanent damage (Figure S1).
 316 We observe more slow-slip events during the immature stage of the fault zone which is
 317 responsible for irregular recurrence intervals for earthquakes. These slow-slip events become
 318 less frequent during the mature stages of the earthquake cycle, and thus there is a more

319 regular sequence of earthquakes. This transition is in accordance with the results from the
320 previous section highlighting the differences between a mature and immature fault damage
321 zone without permanent damage. We show the slip rate range of slow-slip events and fast
322 earthquakes in our simulations, in comparison to those observed on natural faults and in
323 laboratory experiments in Figure 3e. We see that our numerical simulation of a fault zone
324 with healing can produce a wide range of events, both in the fast slipping and slow slipping
325 regime, comparable to those observed along natural faults.

326 4 Discussions and Conclusions

327 Seismologic and geodetic observations in immature fault zones exhibit complex ruptures
328 and distributed coseismic damage. The damage zones in these faults are wider with poorly
329 defined boundaries, resulting in earthquake sequences exhibiting irregular recurrence and
330 size distributions akin to a Gutenberg-Richter magnitude scaling. Examples of such fault
331 zones include the Ridgecrest sequence where geodetic studies have shown complex, multi-
332 fault, and slow rupture with a heterogeneous static stress change (Goldberg et al., 2020).
333 The study by DuRoss et al. (2016) along the immature Wasatch fault zone in Utah suggests
334 partial-segment and multi-segment ruptures with irregular recurrence intervals. Seismic
335 studies after the 2008 earthquake in Peloponnese, Greece have shown negligible surface
336 deformation, i.e., a coseismic slip deficit towards the surface (Feng et al., 2010; Fielding
337 et al., 2009). Dolan and Haravitch (2014) compiled multiple fault zone studies to show
338 that the ratio of the surface slip-measurements to the slip at depth is correlated with fault
339 zone maturity, and immature fault zones tend to have lower ratios. These studies imply
340 that immature fault zones lack surface slip during the coseismic phase and exhibit irregular
341 recurrence intervals, which is also corroborated by our models. In contrast, very mature
342 sections of fault zones have been shown to exhibit higher regularity in earthquake recurrence
343 (e.g., Apline fault in Berryman et al. (2012); Howarth et al. (2021)).

344 Our results unveil how the seismic and aseismic segments in a fault zone interact during
345 the earthquake cycle within an elastic framework. We have shown that the seismogenic zone
346 (velocity-weakening) in our models can have both seismic and aseismic slip episodes, with
347 the latter encompassing slow-slip and creep events. The slow-slip events in our models are
348 distributed within the velocity-weakening segment of the fault and occur throughout the
349 interseismic period. Additionally, we see the aseismic creep penetrating into the velocity-
350 weakening region in our immature fault zone models with healing. Both phenomena con-
351 tribute to the nonuniform release of stresses during the seismic cycle, with slow-slip events
352 having a dominant effect on the earthquake recurrence. Slow-slip events are very challeng-
353 ing to observe in geologically immature strike-slip faults using seismic or geodetic methods.
354 Certain observations along strike-slip fault zones (e.g., the Northern SAF in Murray et al.
355 (2014)) and subduction zones (e.g., Japan subduction zone in K. M. Johnson et al. (2016))
356 have shown seismic and aseismic slip episodes occurring in the nominally velocity-weakening
357 region. As subduction zones tend to be old and mature, some local geologic structures like
358 heterogeneous seafloor structure or complex material properties associated with partially
359 coupled subduction zone might be needed to rejuvenate them (Wang & Bilek, 2014). Sur-
360 face creep has been observed on several fault systems including the Maacama and Bartlett
361 Springs (McFarland et al., 2009; Tong et al., 2013), and creep rates in the shallow parts can
362 be locally very high in the order of $1 \times 10^{-6} \text{ m s}^{-1}$ to $1 \times 10^{-9} \text{ m s}^{-1}$ (Murray et al., 2014).
363 This creep is suggested to extend to depths overlapping with some or all of the seismogenic
364 zone in the Northern San Andreas fault system (Murray et al., 2014). Bruhat and Segall
365 (2017) have explored models where they discuss that the updip propagation of deep inter-
366 seismic creep can explain the slip rate profile along the Northern Cascadia subduction zone.
367 These creep episodes may allude to slow-slip events happening in these regions of immature
368 fault zones as well as subduction zones. Such conditions would be expected to extend the
369 time between major earthquakes, and potentially also limit the earthquake size.

370 To summarize, we performed fully dynamic earthquake cycle simulations in a two-
 371 dimensional strike-slip fault surrounded by an elastic damage zone with time-dependent
 372 shear modulus evolution that emulates coseismic damage and interseismic healing during
 373 seismic and aseismic periods respectively. The models with interseismic healing in imma-
 374 ture fault zones can promote aseismic slip episodes including slow-slip events and creep to
 375 propagate into the seismogenic zone. Our numerical simulations show that such events in
 376 immature fault zones can limit the size of earthquakes and prolong the time between large
 377 earthquakes. In these simulations, slow-slip events are abundant and the stress peaks from
 378 previous earthquakes and slow-slip events are critical in determining the location of and
 379 timing of subsequent events, thereby creating irregularity in recurrence intervals and par-
 380 tial ruptures. These partial ruptures lead to predominantly sub-surface events in immature
 381 fault zones. In contrast, the higher compliance of mature fault zones leads to earthquakes
 382 with complete stress drops and rupture extending throughout the seismogenic zone. We
 383 demonstrate that such fundamental variations in fault-slip behavior can arise due to how
 384 the fault zone structure evolves in time, despite using simple elastic damage zone rheology
 385 and frictional fault properties. Our results emphasize the importance of monitoring seismic
 386 wave velocities and interseismic healing along active faults to help better characterize their
 387 first-order mechanical behavior.

388 Acknowledgments

389 This study was supported by the National Science Foundation (Grant Award EAR-1943742)
 390 and Southern California Earthquake Center (Contribution number 20091). We thank the
 391 editor Dr. German Prieto, the associate editor Dr. Victor Tsai, and the two anonymous
 392 reviewers for their helpful comments. We thank Dr. Roland Burgmann and Dr. Yoshihiro
 393 Kaneko for helpful discussions that significantly improved the quality of this manuscript.
 394 The code used to perform all the numerical simulations are available at: [https://zenodo](https://zenodo.org/record/4898347)
 395 [.org/record/4898347](https://zenodo.org/record/4898347). It is citeable as: "Prithvi Thakur. (2021, June 3). thehalfspace/Sphear: (Version v1.0.0). Zenodo. <http://doi.org/10.5281/zenodo.4898347>".
 396

397 References

- 398 Avouac, J.-P. (2015). From geodetic imaging of seismic and aseismic fault slip to dynamic
 399 modeling of the seismic cycle. *Annual Review of Earth and Planetary Sciences*, *43*,
 400 233–271.
- 401 Barbot, S. (2019a). Modulation of fault strength during the seismic cycle by grain-size
 402 evolution around contact junctions. *Tectonophysics*, *765*, 129–145.
- 403 Barbot, S. (2019b). Slow-slip, slow earthquakes, period-two cycles, full and partial ruptures,
 404 and deterministic chaos in a single asperity fault. *Tectonophysics*, *768*, 228171.
- 405 Barbot, S. (2019c, October). Slow-slip, slow earthquakes, period-two cycles, full and partial
 406 ruptures, and deterministic chaos in a single asperity fault. *Tectonophysics*, *768*,
 407 228171. Retrieved 2021-04-30, from [https://www.sciencedirect.com/science/](https://www.sciencedirect.com/science/article/pii/S0040195119302781)
 408 [article/pii/S0040195119302781](https://www.sciencedirect.com/science/article/pii/S0040195119302781) doi: 10.1016/j.tecto.2019.228171
- 409 Ben-Zion, Y., & Sammis, C. G. (2003). Characterization of fault zones. *Pure and Applied*
 410 *Geophysics*, *160*(3-4), 677–715.
- 411 Berryman, K. R., Cochran, U. A., Clark, K. J., Biasi, G. P., Langridge, R. M., & Villamor,
 412 P. (2012). Major earthquakes occur regularly on an isolated plate boundary fault.
 413 *Science*, *336*(6089), 1690–1693.
- 414 Blanpied, M., Lockner, D., & Byerlee, J. (1991). Fault stability inferred from granite
 415 sliding experiments at hydrothermal conditions. *Geophysical Research Letters*, *18*(4),
 416 609–612.
- 417 Brenguier, F., Campillo, M., Hadziioannou, C., Shapiro, N. M., Nadeau, R. M., & Larose,
 418 E. (2008, September). Postseismic Relaxation Along the San Andreas Fault at Park-
 419 field from Continuous Seismological Observations. *Science*, *321*(5895), 1478–1481.
 420 Retrieved 2021-04-30, from <https://science.sciencemag.org/content/321/5895/>

- 1478 (Publisher: American Association for the Advancement of Science Section:
 Report) doi: 10.1126/science.1160943
- 421
 422 Bruhat, L., & Segall, P. (2017, October). Deformation rates in north-
 423 ern Cascadia consistent with slow updip propagation of deep interseismic
 424 creep. *Geophysical Journal International*, *211*(1), 427–449. Retrieved
 425 2021-04-30, from [http://academic.oup.com/gji/article/211/1/427/4055607/](http://academic.oup.com/gji/article/211/1/427/4055607/Deformation-rates-in-northern-Cascadia-consistent)
 426 [Deformation-rates-in-northern-Cascadia-consistent](http://academic.oup.com/gji/article/211/1/427/4055607/Deformation-rates-in-northern-Cascadia-consistent) doi: 10.1093/gji/ggx317
 427
- Bürgmann, R. (2018). The geophysics, geology and mechanics of slow fault slip. *Earth and
 Planetary Science Letters*, *495*, 112–134.
 428
 429
- Cattania, C. (2019). Complex earthquake sequences on simple faults. *Geophysical Research
 Letters*, *46*(17–18), 10384–10393.
 430
 431
- Chen, K. H., Furumura, T., & Rubinstein, J. (2015). Near-surface versus
 fault zone damage following the 1999 Chi-Chi earthquake: Observa-
 432 tion and simulation of repeating earthquakes. *Journal of Geophysical
 433 Research: Solid Earth*, *120*(4), 2426–2445. Retrieved 2021-04-30, from
 434 <https://agupubs.onlinelibrary.wiley.com/doi/abs/10.1002/2014JB011719>
 435 (_eprint: <https://agupubs.onlinelibrary.wiley.com/doi/pdf/10.1002/2014JB011719>)
 436 doi: <https://doi.org/10.1002/2014JB011719>
 437
- Dieterich, J. H. (1979). Modeling of rock friction: 1. experimental results and con-
 438 stitutive equations. *Journal of Geophysical Research: Solid Earth*, *84*(B5), 2161-
 439 2168. Retrieved from [https://agupubs.onlinelibrary.wiley.com/doi/abs/10](https://agupubs.onlinelibrary.wiley.com/doi/abs/10.1029/JB084iB05p02161)
 440 [.1029/JB084iB05p02161](https://agupubs.onlinelibrary.wiley.com/doi/abs/10.1029/JB084iB05p02161) doi: 10.1029/JB084iB05p02161
 441
 442
- Dolan, J. F., & Haravitch, B. D. (2014, February). How well do surface slip measurements
 track slip at depth in large strike-slip earthquakes? The importance of fault struc-
 443 tural maturity in controlling on-fault slip versus off-fault surface deformation. *Earth
 444 and Planetary Science Letters*, *388*, 38–47. Retrieved 2021-04-30, from [https://](https://www.sciencedirect.com/science/article/pii/S0012821X13006778)
 445 www.sciencedirect.com/science/article/pii/S0012821X13006778 doi: 10.1016/
 446 [j.epsl.2013.11.043](https://www.sciencedirect.com/science/article/pii/S0012821X13006778)
 447
 448
- DuRoss, C. B., Personius, S. F., Crone, A. J., Olig, S. S., Hylland, M. D.,
 449 Lund, W. R., & Schwartz, D. P. (2016). Fault segmentation: New con-
 450 cepts from the Wasatch Fault Zone, Utah, USA. *Journal of Geophysi-
 451 cal Research: Solid Earth*, *121*(2), 1131–1157. Retrieved 2021-04-30, from
 452 <https://agupubs.onlinelibrary.wiley.com/doi/abs/10.1002/2015JB012519>
 453 (_eprint: <https://agupubs.onlinelibrary.wiley.com/doi/pdf/10.1002/2015JB012519>)
 454 doi: <https://doi.org/10.1002/2015JB012519>
 455
- Energetic rupture, coseismic and post-seismic response of the 2008 MW 6.4 Achaia-Elia
 Earthquake in northwestern Peloponnese, Greece: an indicator of an immature trans-
 form fault zone | Geophysical Journal International | Oxford Academic.* (n.d.).
 Retrieved 2021-04-30, from [https://academic.oup.com/gji/article/183/1/103/
 456 591582?login=true](https://academic.oup.com/gji/article/183/1/103/591582?login=true)
 457
 458
- Erickson, B. A., Jiang, J., Barall, M., Lapusta, N., Dunham, E. M., Harris, R., ... others
 (2020). The community code verification exercise for simulating sequences of earth-
 459 quakes and aseismic slip (seas). *Seismological Research Letters*, *91*(2A), 874–890.
 460
- Feng, L., Newman, A. V., Farmer, G. T., Psimoulis, P., & Stiros, S. C. (2010, October).
 Energetic rupture, coseismic and post-seismic response of the 2008 MW 6.4 Achaia-
 461 Elia Earthquake in northwestern Peloponnese, Greece: an indicator of an immature
 462 transform fault zone. *Geophysical Journal International*, *183*(1), 103–110. Retrieved
 463 2021-04-30, from <https://doi.org/10.1111/j.1365-246X.2010.04747.x> doi: 10
 464 [.1111/j.1365-246X.2010.04747.x](https://doi.org/10.1111/j.1365-246X.2010.04747.x)
 465
 466
- Fielding, E. J., Lundgren, P. R., Bürgmann, R., & Funning, G. J. (2009). Shallow fault-zone
 dilatancy recovery after the 2003 bam earthquake in iran. *Nature*, *458*(7234), 64–68.
 467
 468
- Goldberg, D. E., Melgar, D., Sahakian, V. J., Thomas, A. M., Xu, X., Crowell,
 B. W., & Geng, J. (2020). Complex Rupture of an Immature Fault Zone: A
 Simultaneous Kinematic Model of the 2019 Ridgecrest, CA Earthquakes. *Geo-
 469 physical Research Letters*, *47*(3), e2019GL086382. Retrieved 2021-04-30, from
 470
 471
 472
 473
 474
 475

- 476 <https://agupubs.onlinelibrary.wiley.com/doi/abs/10.1029/2019GL086382>
477 (_eprint: <https://agupubs.onlinelibrary.wiley.com/doi/pdf/10.1029/2019GL086382>)
478 doi: <https://doi.org/10.1029/2019GL086382>
- 479 Gratier, J.-P., Favreau, P., & Renard, F. (2003). Modeling fluid transfer along California
480 faults when integrating pressure solution crack sealing and compaction processes.
481 *Journal of Geophysical Research: Solid Earth*, 108(B2). Retrieved 2021-04-30, from
482 <https://agupubs.onlinelibrary.wiley.com/doi/abs/10.1029/2001JB000380>
483 (_eprint: <https://agupubs.onlinelibrary.wiley.com/doi/pdf/10.1029/2001JB000380>)
484 doi: <https://doi.org/10.1029/2001JB000380>
- 485 Harris, R. A., & Day, S. M. (1997). Effects of a low-velocity zone on a dynamic rupture.
486 *Bulletin of the Seismological Society of America*, 87(5), 1267–1280.
- 487 Heaton, T. H. (1990, November). Evidence for and implications of self-healing pulses of slip
488 in earthquake rupture. *Physics of the Earth and Planetary Interiors*, 64(1), 1–20. Re-
489 trieved 2021-04-30, from [https://www.sciencedirect.com/science/article/pii/](https://www.sciencedirect.com/science/article/pii/003192019090002F)
490 [003192019090002F](https://www.sciencedirect.com/science/article/pii/003192019090002F) doi: 10.1016/0031-9201(90)90002-F
- 491 Heimisson, E. R. (2020). Crack to pulse transition and magnitude statistics during earth-
492 quake cycles on a self-similar rough fault. *Earth and Planetary Science Letters*, 537,
493 116202.
- 494 Howarth, J. D., Barth, N. C., Fitzsimons, S. J., Richards-Dinger, K., Clark, K. J., Biasi,
495 G. P., ... Sutherland, R. (2021). Spatiotemporal clustering of great earthquakes on
496 a transform fault controlled by geometry. *Nature Geoscience*, 14(5), 314–320.
- 497 Huang, Y., & Ampuero, J.-P. (2011a). Pulse-like ruptures induced by low-
498 velocity fault zones. *Journal of Geophysical Research: Solid Earth*, 116(B12).
499 Retrieved from [https://agupubs.onlinelibrary.wiley.com/doi/abs/10.1029/](https://agupubs.onlinelibrary.wiley.com/doi/abs/10.1029/2011JB008684)
500 [2011JB008684](https://agupubs.onlinelibrary.wiley.com/doi/abs/10.1029/2011JB008684) doi: 10.1029/2011JB008684
- 501 Huang, Y., & Ampuero, J.-P. (2011b). Pulse-like ruptures induced by
502 low-velocity fault zones. *Journal of Geophysical Research: Solid*
503 *Earth*, 116(B12). Retrieved 2021-04-30, from <https://agupubs>
504 [.onlinelibrary.wiley.com/doi/abs/10.1029/2011JB008684](https://agupubs.onlinelibrary.wiley.com/doi/abs/10.1029/2011JB008684) (_eprint:
505 <https://agupubs.onlinelibrary.wiley.com/doi/pdf/10.1029/2011JB008684>) doi:
506 <https://doi.org/10.1029/2011JB008684>
- 507 Huang, Y., Ampuero, J.-P., & Helmberger, D. V. (2014a). Earthquake rup-
508 tures modulated by waves in damaged fault zones. *Journal of Geophysi-
509 cal Research: Solid Earth*, 119(4), 3133–3154. Retrieved 2021-04-30, from
510 <https://agupubs.onlinelibrary.wiley.com/doi/abs/10.1002/2013JB010724>
511 (_eprint: <https://agupubs.onlinelibrary.wiley.com/doi/pdf/10.1002/2013JB010724>)
512 doi: <https://doi.org/10.1002/2013JB010724>
- 513 Huang, Y., Ampuero, J.-P., & Helmberger, D. V. (2014b). Earthquake ruptures modulated
514 by waves in damaged fault zones. *Journal of Geophysical Research: Solid Earth*,
515 119(4), 3133–3154.
- 516 Idini, B., & Ampuero, J.-P. (2020a). Fault-Zone Damage Promotes Pulse-Like
517 Rupture and Back-Propagating Fronts via Quasi-Static Effects. *Geophysi-
518 cal Research Letters*, 47(23), e2020GL090736. Retrieved 2021-04-30, from
519 <https://agupubs.onlinelibrary.wiley.com/doi/abs/10.1029/2020GL090736>
520 (_eprint: <https://agupubs.onlinelibrary.wiley.com/doi/pdf/10.1029/2020GL090736>)
521 doi: <https://doi.org/10.1029/2020GL090736>
- 522 Idini, B., & Ampuero, J.-P. (2020b). Fault-zone damage promotes pulse-like rupture and
523 rapid-tremor-reversals.
- 524 Johnson, K. M., Mavrommatis, A., & Segall, P. (2016). Small interseismic asperiti-
525 es and widespread aseismic creep on the northern Japan subduction interface.
526 *Geophysical Research Letters*, 43(1), 135–143. Retrieved 2021-04-30, from
527 <https://agupubs.onlinelibrary.wiley.com/doi/abs/10.1002/2015GL066707>
528 (_eprint: <https://agupubs.onlinelibrary.wiley.com/doi/pdf/10.1002/2015GL066707>)
529 doi: <https://doi.org/10.1002/2015GL066707>

- 530 Johnson, P. A., & Jia, X. (2005, October). Nonlinear dynamics, granular media and
531 dynamic earthquake triggering. *Nature*, *437*(7060), 871–874. Retrieved 2021-04-30,
532 from <https://www.nature.com/articles/nature04015> (Number: 7060 Publisher:
533 Nature Publishing Group) doi: 10.1038/nature04015
- 534 Kaneko, Y., Ampuero, J.-P., & Lapusta, N. (2011, October). Spectral-element simulations of
535 long-term fault slip: Effect of low-rigidity layers on earthquake-cycle dynamics. *Jour-
536 nal of Geophysical Research (Solid Earth)*, *116*, B10313. doi: 10.1029/2011JB008395
- 537 Kaneko, Y., Lapusta, N., & Ampuero, J.-P. (2008). Spectral element modeling of spon-
538 taneous earthquake rupture on rate and state faults: Effect of velocity-strengthening
539 friction at shallow depths. *Journal of Geophysical Research: Solid Earth*, *113*(B9).
- 540 Kaproth, B. M., & Marone, C. (2014). Evolution of elastic wave speed during
541 shear-induced damage and healing within laboratory fault zones. *Journal of Geo-
542 physical Research: Solid Earth*, *119*(6), 4821–4840. Retrieved 2021-04-30, from
543 <https://agupubs.onlinelibrary.wiley.com/doi/abs/10.1002/2014JB011051>
544 (_eprint: <https://agupubs.onlinelibrary.wiley.com/doi/pdf/10.1002/2014JB011051>)
545 doi: <https://doi.org/10.1002/2014JB011051>
- 546 Lapusta, N., & Rice, J. R. (2003). Nucleation and early seismic propagation of small and
547 large events in a crustal earthquake model. *Journal of Geophysical Research: Solid
548 Earth*, *108*(B4).
- 549 Lapusta, N., Rice, J. R., Ben-Zion, Y., & Zheng, G. (2000). Elastodynamic analysis
550 for slow tectonic loading with spontaneous rupture episodes on faults with rate- and
551 state-dependent friction. *Journal of Geophysical Research: Solid Earth*, *105*(B10),
552 23765–23789. Retrieved from [https://agupubs.onlinelibrary.wiley.com/doi/
553 abs/10.1029/2000JB900250](https://agupubs.onlinelibrary.wiley.com/doi/abs/10.1029/2000JB900250) doi: 10.1029/2000JB900250
- 554 Lewis, M., Peng, Z., Ben-Zion, Y., & Vernon, F. (2005). Shallow seismic trapping structure
555 in the san jacinto fault zone near anza, california. *Geophysical Journal International*,
556 *162*(3), 867–881.
- 557 Lewis, M. A., & Ben-Zion, Y. (2010). Diversity of fault zone damage and trapping structures
558 in the parkfield section of the san andreas fault from comprehensive analysis of near
559 fault seismograms. *Geophysical Journal International*, *183*(3), 1579–1595.
- 560 Li, Y., Brgmann, R., & Zhao, B. (2020, January). Evidence of Fault Immaturity from
561 Shallow Slip Deficit and Lack of Postseismic Deformation of the 2017 Mw6.5 Ji-
562 uzhaigou Earthquake. *Bulletin of the Seismological Society of America*, *110*(1),
563 154–165. Retrieved 2021-04-30, from <https://doi.org/10.1785/0120190162> doi:
564 10.1785/0120190162
- 565 Li, Y.-G., Chen, P., Cochran, E. S., Vidale, J. E., & Burdette, T. (2006a). Seismic evidence
566 for rock damage and healing on the san andreas fault associated with the 2004 m
567 6.0 parkfield earthquake. *Bulletin of the Seismological Society of America*, *96*(4B),
568 S349–S363.
- 569 Li, Y.-G., Chen, P., Cochran, E. S., Vidale, J. E., & Burdette, T. (2006b, September).
570 Seismic Evidence for Rock Damage and Healing on the San Andreas Fault Associ-
571 ated with the 2004 M 6.0 Parkfield Earthquake. *Bulletin of the Seismological Soci-
572 ety of America*, *96*(4B), S349–S363. Retrieved 2021-04-30, from [https://doi.org/
573 10.1785/0120050803](https://doi.org/10.1785/0120050803) doi: 10.1785/0120050803
- 574 Li, Y.-G., Vidale, J. E., Day, S. M., Oglesby, D. D., & Cochran, E. (2003, April). Postseis-
575 mic Fault Healing on the Rupture Zone of the 1999 M 7.1 Hector Mine, California,
576 Earthquake. *Bulletin of the Seismological Society of America*, *93*(2), 854–869. Re-
577 trieved 2021-04-30, from [https://pubs.geoscienceworld.org/ssa/bssa/article/
578 93/2/854/120884/Postseismic-Fault-Healing-on-the-Rupture-Zone-of](https://pubs.geoscienceworld.org/ssa/bssa/article/93/2/854/120884/Postseismic-Fault-Healing-on-the-Rupture-Zone-of) (Pub-
579 lisher: GeoScienceWorld) doi: 10.1785/0120020131
- 580 Lyakhovskiy, V., Ben-Zion, Y., & Agnon, A. (2005). A viscoelastic damage rheology and
581 rate-and state-dependent friction. *Geophysical Journal International*, *161*(1), 179–
582 190.
- 583 McFarland, F. S., Lienkaemper, J. J., & Caskey, S. J. (2009). *Data from theodolite measure-
584 ments of creep rates on San Francisco Bay region faults, California, 1979-2012* (USGS

- 585 Numbered Series No. 2009-1119). Reston, VA: U.S. Geological Survey. Retrieved 2021-
586 04-30, from <http://pubs.er.usgs.gov/publication/ofr20091119> (Code Number:
587 2009-1119 Code: Data from theodolite measurements of creep rates on San Francisco
588 Bay region faults, California, 1979-2012 Publication Title: Data from theodolite mea-
589 surements of creep rates on San Francisco Bay region faults, California, 1979-2012 Re-
590 porter: Data from theodolite measurements of creep rates on San Francisco Bay region
591 faults, California, 1979-2012 Series: Open-File Report) doi: 10.3133/ofr20091119
- 592 Mizuno, T., Kuwahara, Y., Ito, H., & Nishigami, K. (2008). Spatial variations in fault-zone
593 structure along the nojima fault, central japan, as inferred from borehole observations
594 of fault-zone trapped waves. *Bulletin of the Seismological Society of America*, *98*(2),
595 558–570.
- 596 Murray, J. R., Minson, S. E., & Svarc, J. L. (2014). Slip rates and spatially vari-
597 able creep on faults of the northern San Andreas system inferred through
598 Bayesian inversion of Global Positioning System data. *Journal of Geophys-
599 ical Research: Solid Earth*, *119*(7), 6023–6047. Retrieved 2021-04-30, from
600 <https://agupubs.onlinelibrary.wiley.com/doi/abs/10.1002/2014JB010966>
601 (eprint: <https://agupubs.onlinelibrary.wiley.com/doi/pdf/10.1002/2014JB010966>)
602 doi: <https://doi.org/10.1002/2014JB010966>
- 603 Okubo, K., Bhat, H. S., Rougier, E., Marty, S., Schubnel, A., Lei, Z., . . . Klinger, Y. (2019).
604 Dynamics, radiation, and overall energy budget of earthquake rupture with coseismic
605 off-fault damage. *Journal of Geophysical Research: Solid Earth*.
- 606 Pei, S., Niu, F., Ben-Zion, Y., Sun, Q., Liu, Y., Xue, X., . . . Shao, Z. (2019, May).
607 Seismic velocity reduction and accelerated recovery due to earthquakes on the Long-
608 menshan fault. *Nature Geoscience*, *12*(5), 387–392. Retrieved 2021-04-30, from
609 <https://www.nature.com/articles/s41561-019-0347-1> (Number: 5 Publisher:
610 Nature Publishing Group) doi: 10.1038/s41561-019-0347-1
- 611 Peng, Z., & Ben-Zion, Y. (2006, March). Temporal Changes of Shallow Seismic Velocity
612 Around the Karadere-Dzce Branch of the North Anatolian Fault and Strong Ground
613 Motion. *pure and applied geophysics*, *163*(2), 567–600. Retrieved 2021-04-30, from
614 <https://doi.org/10.1007/s00024-005-0034-6> doi: 10.1007/s00024-005-0034-6
- 615 Perrin, C., Manighetti, I., Ampuero, J.-P., Cappa, F., & Gaudemer, Y. (2016). Location
616 of largest earthquake slip and fast rupture controlled by along-strike change in fault
617 structural maturity due to fault growth. *Journal of Geophysical Research: Solid Earth*,
618 *121*(5), 3666–3685. Retrieved from [https://agupubs.onlinelibrary.wiley.com/
619 doi/abs/10.1002/2015JB012671](https://agupubs.onlinelibrary.wiley.com/doi/abs/10.1002/2015JB012671) doi: 10.1002/2015JB012671
- 620 Rice, J. R. (1993). Spatio-temporal complexity of slip on a fault. *Journal of Geophysical
621 Research: Solid Earth*, *98*(B6), 9885–9907.
- 622 Rice, J. R., & Ben-Zion, Y. (1996). Slip complexity in earthquake fault models. *Proceedings
623 of the National Academy of Sciences*, *93*(9), 3811–3818.
- 624 Roux, P., & Ben-Zion, Y. (2014). Monitoring fault zone environments with correlations of
625 earthquake waveforms. *Geophysical Journal International*, *196*(2), 1073–1081. (Pub-
626 lisher: Oxford University Press)
- 627 Rubinstein, J. L., & Beroza, G. C. (2005). Depth constraints on nonlinear strong ground
628 motion from the 2004 parkfield earthquake. *Geophysical Research Letters*, *32*(14).
- 629 Ruina, A. (1983). Slip instability and state variable friction laws. *Journal of Geophys-
630 ical Research: Solid Earth*, *88*(B12), 10359–10370. Retrieved from [https://agupubs
631 .onlinelibrary.wiley.com/doi/abs/10.1029/JB088iB12p10359](https://agupubs.onlinelibrary.wiley.com/doi/abs/10.1029/JB088iB12p10359) doi: 10.1029/
632 JB088iB12p10359
- 633 Scholz, C. H. (1998). Earthquakes and friction laws. *Nature*, *391*(6662), 37.
- 634 Snieder, R., Sens-Schönfelder, C., Ruigrok, E., & Shiomi, K. (2016). Seismic shear waves
635 as focault pendulum. *Geophysical Research Letters*, *43*(6), 2576–2581.
- 636 Taira, T., Silver, P. G., Niu, F., & Nadeau, R. M. (2009, October). Remote triggering of
637 fault-strength changes on the San Andreas fault at Parkfield. *Nature*, *461*(7264), 636–
638 639. Retrieved 2021-04-30, from <https://www.nature.com/articles/nature08395>
639 (Number: 7264 Publisher: Nature Publishing Group) doi: 10.1038/nature08395

- 640 Thakur, P., Huang, Y., & Kaneko, Y. (2020, August). Effects of LowVelocity Fault
641 Damage Zones on LongTerm Earthquake Behaviors on Mature StrikeSlip Faults.
642 *Journal of Geophysical Research: Solid Earth*, 125(8). Retrieved 2021-04-30, from
643 <https://onlinelibrary.wiley.com/doi/10.1029/2020JB019587> doi: 10.1029/
644 2020JB019587
- 645 Tong, X., Sandwell, D. T., & SmithKonter, B. (2013). High-resolution interseismic
646 velocity data along the San Andreas Fault from GPS and InSAR. *Journal of*
647 *Geophysical Research: Solid Earth*, 118(1), 369–389. Retrieved 2021-04-30, from
648 <https://agupubs.onlinelibrary.wiley.com/doi/abs/10.1029/2012JB009442>
649 (_eprint: <https://agupubs.onlinelibrary.wiley.com/doi/pdf/10.1029/2012JB009442>)
650 doi: <https://doi.org/10.1029/2012JB009442>
- 651 Tsai, V. C., & Hirth, G. (2020). Elastic impact consequences for high-frequency earthquake
652 ground motion. *Geophysical Research Letters*, 47(5), e2019GL086302.
- 653 Vidale, J. E., & Li, Y.-G. (2003, January). Damage to the shallow Landers fault from the
654 nearby Hector Mine earthquake. *Nature*, 421(6922), 524–526. Retrieved 2021-04-30,
655 from <https://www.nature.com/articles/nature01354> (Number: 6922 Publisher:
656 Nature Publishing Group) doi: 10.1038/nature01354
- 657 Waldhauser, F., & Ellsworth, W. L. (2002). Fault structure and mechanics of the hayward
658 fault, california, from double-difference earthquake locations. *Journal of Geophysical*
659 *Research: Solid Earth*, 107(B3), ESE–3.
- 660 Wang, K., & Bilek, S. L. (2014). Invited review paper: Fault creep caused by subduction
661 of rough seafloor relief. *Tectonophysics*, 610, 1–24.
- 662 Wu, C., Peng, Z., & Ben-Zion, Y. (2009, January). Non-linearity and temporal changes of
663 fault zone site response associated with strong ground motion. *Geophysical Journal*
664 *International*, 176(1), 265–278. Retrieved 2021-04-30, from [https://doi.org/10](https://doi.org/10.1111/j.1365-246X.2008.04005.x)
665 [.1111/j.1365-246X.2008.04005.x](https://doi.org/10.1111/j.1365-246X.2008.04005.x) doi: 10.1111/j.1365-246X.2008.04005.x
- 666 Zhao, P., & Peng, Z. (2009). Depth extent of damage zones around the central calaveras fault
667 from waveform analysis of repeating earthquakes. *Geophysical Journal International*,
668 179(3), 1817–1830.